Journal of Archaeological Science: Reports 30 (2020) 102254

Contents lists available at ScienceDirect

Journal of Archaeological Science: Reports

journal homepage: www.elsevier.com/locate/jasrep

White on blue: A study on underglaze-decorated ceramic tiles from 15th-16th-century Valencian and Sevillian productions

S. Coentro[a,b,*], L.C. Alves[c], J. Coll Conesa[d], T. Ferreira[e], J. Mirão[f], R.C. da Silva[g], R. Trindade[h], V.S.F. Muralha[a,†]

[a] VICARTE – Research Unit "Glass and Ceramic for the Arts", FCT, Caparica Campus, Universidade NOVA de Lisboa, 2829-516 Caparica, Portugal
[b] Departamento de Conservação e Restauro, FCT, Caparica Campus, Universidade NOVA de Lisboa, 2829-516 Caparica, Portugal
[c] C2TN-IST/UL, Centro de Ciências e Tecnologias Nucleares, Instituto Superior Técnico, Universidade de Lisboa, Estrada Nacional 10, 2695-066 Bobadela, Portugal
[d] Museo Nacional de Cerámica y Artes Suntuarias "González Martí", Poeta Querol, 2, 46002 – Valencia, España
[e] Departamento de Química, Escola de Ciência e Tecnologia, Laboratório HERCULES, Universidade de Évora, Largo Marquês de Marialva, 8, 7000-809 Évora, Portugal
[f] Departamento de Geociências, Escola de Ciência e Tecnologia, Laboratório HERCULES, Universidade de Évora, Largo Marquês de Marialva, 8, 7000-809 Évora, Portugal
[g] IPFN-IST/UL, Instituto de Plasmas e Fusão Nuclear, Instituto Superior Técnico, Universidade de Lisboa, Estrada Nacional 10, 2695-066 Bobadela, Portugal
[h] Museu Nacional de Arte Antiga (MNAA), Rua das Janelas Verdes, 1249-017 Lisboa, Portugal

ARTICLE INFO

Keywords:
Cobalt
Underglaze
Tin glaze
Ceramic tile

ABSTRACT

This study characterises and compares tin-opacified underglaze-decorated tiles from Valencian and Sevillian provenances. This technique, where the cobalt and manganese pigments are applied below an opaque white glaze, was used in the Iberian Peninsula between the 14th and early 16th centuries. The chemical and morphological characterisation of the glazes was performed by Optical Microscopy (OM), Scanning Electron Microscopy with Energy-Dispersive X-Ray Spectroscopy (SEM-EDS), μ-Raman Spectroscopy, and μ-Particle-Induced X-Ray Emission (μ-PIXE). Both the morphology of the glazes and their chemical composition allowed for the distinction between the two production centres. Sevillian glazes exhibit a thicker pigment layer, as well as higher SnO_2 and lower K_2O contents than the Valencian ones. Furthermore, the SEM analysis of cobalt pigment particles identified an interior nucleus rich in Co, Fe and Ni, and an exterior layer rich in Si, Ca, Mg and Na, suggesting that the pigment was used mixed with clay or sand.

1. Introduction

1.1. Underglaze-decorated ceramics

Underglaze implies that the painting layer of the ceramic object is located under a glaze layer, which acts like a varnish to fixate the pigments and to give a homogenous and brilliant finish to the surface. This technique has been documented in Islamic ceramics as early as the 9th century, *i.e.*, in Raqqada (Ben Amara et al., 2011) and Palermo (Arcifa and Bagnera, 2018).

The mutual influence between Islam and China is believed to have driven the development of stonepaste (or fritware) technology, which provided a white background on which the pigments were directly applied and then covered with a transparent glaze, eliminating the need for a white slip or white-firing clays to achieve a porcelain-like appearance (Tite et al., 2011; Watson, 2004). In parallel, tin-opacified ceramics were also developed since the 8th century in Egypt and the Levant (Matin et al., 2018), and introduced in the Iberian Peninsula between the last quarter of the 9th century and the first quarter of the 10th century (Salinas and Pradell, 2018).

The Islamic presence in the Iberian Peninsula between the 8th and the 15th centuries provided a specific background for the development of important ceramic centres. Tin-opacified glazes were among the most significant innovations brought by the Islamic potters, along with the cobalt blue pigment, which became inseparable from the architectural tile until our days (Martínez Caviró, 1991). During the 14th century, a different type of underglaze painting was developed: instead of a transparent glaze (like the one used in stonepaste or fritware ceramics), this type used a white tin-opacified glaze over the painted decorations. Archaeological evidence has shown that in Valencian blue-and-white underglaze-decorated ceramics, the cobalt pigment was applied onto the raw ceramic object, which was then fired for the first time.

* Corresponding author.
E-mail address: scoentro@fct.unl.pt (S. Coentro).
† In memoriam of our co-author and dear friend V.S.F. Muralha.

https://doi.org/10.1016/j.jasrep.2020.102254
Received 15 October 2019; Received in revised form 21 January 2020; Accepted 30 January 2020
Available online 27 March 2020
2352-409X/

Afterwards, a white lead–tin glaze frit was applied over the painted object, which was then was fired a second time (Coll Conesa, 2009a). This technology has also been documented in 14th-century Nasrid Granada, where ceramic fragments were found decorated with cobalt oxide prior to having been coated with a tin-glaze frit (García-Porras 2012).

The beginnings of this specific opaque underglaze technique or the reasons for its use are not clear. Their highlight was in 15th-century Valencia (Spain), already under Christian ruling, albeit with many Islamic potters in the region (Coll Conesa, 2009b). Matin et al. (2018) have shown that several early Islamic tin-opacified wares were overglaze-decorated, including green-and-brown and blue-and-white ceramics from Raqqa and Samarra, respectively. The closest Islamic parallel to the Hispano-Moresque underglaze technology documented unequivocally in the literature concerns Sicilian 9th-10th-century shards that were decorated with copper green and manganese brown under an opaque glaze, although this glaze is not tin-opacified. Instead, it contains quartz (SiO_2) crystals that render it opaque with a matt appearance (Testolini 2018).

In the Iberian Peninsula, an underglaze tin-opacified cobalt blue decoration has been documented in Granada (García-Porras 2012), Valencia (Roldán et al., 2006), Catalonia (Pradell et al., 2010), Teruel (Pérez-Arantegui et al., 2009b), and Seville (Pleguezuelo 2011). Contrary to blue-and-white ceramics, tin-opacified "green and brown" Islamic and Hispano-Moresque wares exhibit overglaze decorations throughout the Iberian Peninsula, except for one (so far) set of Catalonian ceramics dated from the 14th century (Salinas et al., 2017).

The Valencian and Sevillian regions were among the most important production centres of Hispano-Moresque ceramics. While in Valencia the underglaze technique was the most used one for decorating ceramic tiles, in Seville the *cuerda seca* and the *arista* techniques were more popular (Martínez Caviró, 1991). Nevertheless, during a recent study on Hispano-Moresque tiles (Coentro, 2017), an underglaze decoration was identified in shards attributed to a Sevillian production. Opposing to what has been written about Valencia, underglaze-decorated Sevillian ceramics were yet to be studied.

1.2. Study objectives

The main objective of this work is to compare Valencian and Sevillian tin-opacified underglaze-decorated architectural tiles in order to identify and characterise different underglaze decoration techniques from different provenances with tin-opacified glazes as a common feature. Furthermore, Co-rich inclusions are analised in detail by SEM-EDS, giving clues to the original raw material.

2. Materials and methods

2.1. Sample description

Fourteen tiles (Fig. 1) from three different institutions – Monastery of Santa Clara-a-Velha, Coimbra, Portugal (SCV); Museo de Cerámica "González Martí", Valencia, Spain (MCV); Instituto Valencia de Don Juan, Madrid, Spain (IVDJ-S) – were studied. Table 1 contains the list of the tiles with information on their decoration technique, provenance and chronology.

These samples comprise different decorative techniques: flat (the glaze exhibits a flat surface), *arista* (different-coloured glazes are physically separated by ridged ceramic lines), and "low-*arista*" (slightly ridged ceramic lines, yet covered with the white glaze, mark the outlines of the drawing). The MCV samples in this study exhibit flat surfaces with hand-drawn blue (and occasionally brown) decorations, whereas the decoration contours in SCV and IVDJ-S samples have been printed in the clay by means of ridged lines, suggesting a simplification of the production process. A schematic representation of the decorative techniques is presented in Fig. 2.

The sampling procedure consisted of collecting very small samples (*ca.* 2 mm wide) from fractured areas where the visual impact is practically imperceptible. Samples were then mounted as cross-sections in epoxy resin (Araldite® 2020) and polished in Micro-Mesh® sheets up to grit 4000.

2.2. Analytical techniques

All the analyses were performed on the same cross-section samples, which was possible due to the non-destructive character of the chosen techniques. The samples were first observed by optical microscopy (OM), followed by the chemical characterisation of the glazes by μ-PIXE. SEM-EDS was used to both chemically and morphologically characterise the glazes, the glaze-ceramic interface and the inclusions that were observed. Finally, μ-Raman was used for the identification of the inclusions present in the glaze.

2.3. Equipment specifications

2.3.1. OM

Optical Microscopy was carried out using a Zeiss Axioplan 2 microscope equipped with × 5, ×20, ×50 and × 100 magnification objectives in polarised light and dark field mode. The images were recorded with a Nikon digital camera DXM1200F camera coupled to the microscope.

2.3.2. μ-Raman

The equipment used is a Labram 300 Jobin Yvon spectrometer, equipped with a solid-state laser of 500 mW power (532 nm) and a He-Ne laser of 17 mW power (633 nm). A 50x or a 100x Olympus objective lens was used to focus the laser beam. The laser power was filtered to 10% incident power using a neutral density filter for all analyses. The LabSpec software (v 5.15.25) was used to determine the exact peak wavenumbers. Except when stated otherwise, the RRUFF database project on minerals (RRUFF, 2018) was used for the attribution of the Raman spectra. The analysis were performed at the Department of Conservation and Restoration at Faculty of Sciences and Technology – NOVA University of Lisbon, Potugal.

2.3.3. μ-PIXE

The analyses were performed with the Oxford Microbeams OM150 type scanning nuclear microprobe installed at one of the beam lines of the 2.5 MV Van de Graaff accelerator at the Nuclear and Technological Campus of IST-UL. The used vacuum experimental setup comprises a 30 mm^2 SDD X-ray detector and the ability of focusing the used 1 MeV proton beam down to 3 × 4 μm^2 while scanning the beam up to a 3730 × 3730 μm^2 sample area. Allowing to obtain 2D elemental distribution maps these were used to identify the glaze layer and select representative regions of interest for further quantitative analysis. Operation and data manipulation were achieved with the OMDAQ software code (Grime and Dawson, 1995), and quantitative data analysis performed with the GUPIXWIN programme (Campbell et al., 2010). The results were validated through the quantitative analysis of two glass reference standards (Corning Museum of Glass B and C) (Table 2).

2.3.4. SEM-EDS

A variable pressure scanning electron microscope HITACHI S-3700N in the backscattering mode was used for SEM imaging. The microscope is coupled with a Brüker Xflash 5010 SDD energy dispersive X-ray spectrometer, used for elemental point analysis and mapping with an acceleration voltage of 20 kV. Samples were analysed in cross-sections under an air pressure of 40 Pa. The resolution of the EDS detector is 123 eV at the Mn Kα line energy. Esprit1.9 software from Brüker Corporation was used for EDS tasks and quantification. The SEM-EDS study was carried out at HERCULES Laboratory, in University of Évora, Portugal.

Fig. 1. Studied samples from Monastery of Santa Clara-a-Velha, Coimbra, Portugal (**SCV**); Museo de Cerámica "González Martí", Valencia, Spain (**MCV**); Instituto Valencia de Don Juan, Madrid, Spain (**IVDJ-S**).

Table 1
List of samples with information on the decoration technique, provenance and chronology.

sample	decoration	location	provenance	chronology
MCV 2-1T	Flat with white and blue	Museo de Cerámica "González Martí", Valencia, Spain	Paterna/Manises (Valencia)	15th century
MCV 3-1R				
MCV 1-1R	Flat with white, blue and brown			
MCV 4-1G				
MCV 4-2G				
MCV 8-1G				
MCV 8-2G				
MCV 8-3G				
IVDJ-S 4134	*Arista* with white, blue and lustre	Instituto Valencia de Don Juan, Madrid, Spain	Seville	early 16th century
IVDJ-S 4185				
SCV 34Ei4068	"low" arista with white and blue (and lustre?)	Monastery of Santa Clara-a-Velha, Coimbra, Portugal	Seville (attributed)	early 16th century
SCV 494i4327				
SCV 49-15F4338				
SCV 51-1M4467	Relief with white and blue			

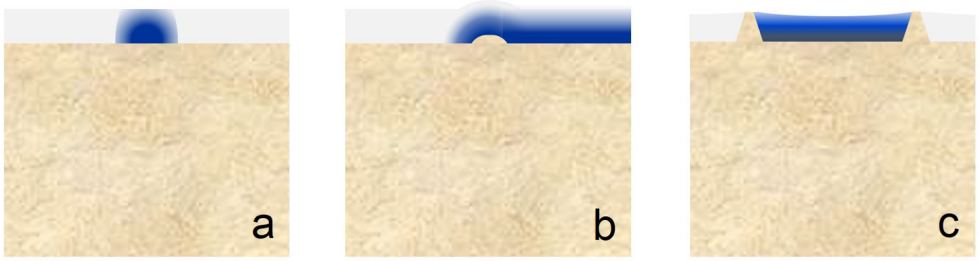

Fig. 2. Schematic representation of the different types of underglaze decoration observed, according to the decoration technique: **(a)** flat (MCV); **(b)** "low-*arista*" (SCV) – small ridge marking the outlines; **(c)** *arista* (IVDJ-S) – pronounced ridges separate the different-coloured glazes.

Table 2
Chemical composition of glass standards Corning Museum of Glass (CMoG) B and C: certified (Brill, 1999) and average (n = 9) measured by μ-PIXE.

	Na_2O	MgO	Al_2O_3	SiO_2	K_2O	CaO	TiO_2
CMoG B							
Certified (wt.%)	17.0	1.03	4.36	62.3	1.00	8.56	0.089
Measured by μ-PIXE (wt.%)	17.1	0.96	4.29	64.8	0.96	7.53	0.12
RSD (%)	7.3	5.7	6.9	1.6	5.4	4.9	17.9
CMoG C							
Certified (wt.%)	1.07	2.76	0.87	34.3	2.84	5.07	0.79
Measured by μ-PIXE (wt.%)	1.14	2.36	0.89	35.8	2.60	4.42	0.55
RSD (%)	7.7	5.2	4.9	3.7	2.2	1.7	19.4

	MnO	Fe_2O_3	CoO	NiO	CuO	BaO	PbO
CMoG B							
Certified (wt.%)	0.25	0.34	0.046	0.099	2.66	0.12	0.61
Measured by μ-PIXE (wt.%)	0.22	0.30	0.08	0.10	2.30	0.10	0.43
RSD (%)	18.3	10.9	36.7	21.2	7.7	40.2	29.8
CMoG C							
Certified (wt.%)	–	0.34	0.18	–	1.13	11.4	36.7
Measured by μ-PIXE (wt.%)	–	0.30	0.16	–	1.09	11.5	38.8
RSD (%)	–	6.4	18.5	–	5.8	1.6	4.6

RSD – relative standard deviation.

3. Results

3.1. Observations by Optical Microscopy

The underglaze decoration technique is identified by OM through the dark layer corresponding to the cobalt blue (Fig. 3*a, 3c-d*) or manganese brown (Fig. 3*b*) pigment between the tin-opacified glaze and the ceramic body. In some cases, a colour gradient from darker to lighter blue is also observed from the interface to the surface of the glaze (Fig. 3a and c). Among the studied samples, two groups were differentiated according to the thickness of the pigment layer:

- *Type 1* exhibits a thin blue pigment layer (*ca.* 30–50 μm) and corresponds to MCV samples (Fig. 3*a*). Brown decorations exhibit irregular dark agglomerates measuring up to *ca.* 50 μm, also located at the glaze-ceramic interface (Fig. 3*b*).
- *Type 2* exhibits a thicker pigment layer (> 100 μm) and includes IVDJ-S and SCV samples (both attributed to Seville) (Fig. 3*c and 3d*).

3.2. SEM-EDS analysis

The morphological observation by SEM added some distinguishing features between the previously mentioned glaze *Types 1* and *2*:

- *Type 1* (Fig. 4) exhibits small Co– or Mn-containing particles (< 15 μm) scarcely distributed near the glaze-ceramic interface in blue and brown glazes, respectively. A very homogeneous tin-opacified glaze with very small and well-distributed cassiterite agglomerates is observed. Bubbles and mineral inclusions (other than the mentioned Co-rich ones) are scarce.
- *Type 2* (Fig. 5) exhibits a clear morphological difference between the two layers observed in the glaze – the lower layer is composed of many inclusions related to the Co pigment, whereas the upper layer is more homogeneous and similar to the MCV glazes with its well-distributed tin oxide agglomerates. These are, however, larger in size in SCV and IVDJ-S samples, suggesting less grinding of the glaze frit.

SEM-EDS allowed the analysis of the cobalt pigment both in *Type 1* and *Type 2* glazes. The smaller dimensions of the Co-inclusions in MCV glazes (< 15 μm) required higher magnifications than those necessary to identify them in SCV and IVDJ-S glazes where, not only the pigment layer is thicker, but cobalt inclusions are larger (up to 40 μm). However, EDS analysis revealed similar results for all samples, with a predominance of Co, Fe and Ni in these inclusions. The EDS map in Fig. 5*d* illustrates how these elements occasionally distributed within different Co-particles, something that has been reported in the literature for other cobalt blue glazes (Coentro et al., 2018; Guilherme et al., 2014; Zucchiatti et al., 2006). The fact that the SEM-EDS equipment irradiates an area of approximately 4 μm^2 makes it difficult to perform a detailed analysis within each inclusion, although in an MCV particle it was possible to distinguish a Ni-rich nucleus and Co homogenously spread (Fig. 4*c*). Also, Fe is heterogeneously spread within this particle, and an outside layer was clearly observed richer in Ca, Mg, Si and Na.

Fig. 5*b* displays the EDS spectra of two areas in the different glaze layers in sample SCV 49-15F4338. The upper layer (corresponding to the tin-opacified glaze) shows higher Si and Pb peaks. Tin is only detected in this layer. On the other hand, the lower layer shows, as expected, higher intensity peaks related to the cobalt pigment – Fe, Co, Ni – and higher Al.

3.3. μ-Raman analysis

The μ-Raman analysis of the pigment particles in blue glazes identified two different spectra consistent with ferrite spinels (Fig. 6). One spectrum exhibits two strong bands at *ca.* 487 cm^{-1} and *ca.* 704 cm^{-1} (Fig. 6*a*), and the other exhibits these bands with slightly different values: *ca.* 472 cm^{-1} and *ca.* 698 cm^{-1} (Fig. 6*b*). The first values are reported in the literature for both nickel ferrites ($NiFe_2O_4$) (Kamble et al., 2015) and cobalt ferrites ($CoFe_2O_4$) (Chandramohan et al., 2011; Majumdar, 2012), whereas the latter are reported for nickel ferrites (Kim et al., 2014). The band at *ca.* 668 cm^{-1} is consistent with magnetite (RRUFF, 2018). No association was evident between the identified spectra and a specific set of samples.

The dark inclusions observed in brown-coloured glazes were identified by μ-Raman as braunite ($Mn^{2+}Mn_6^{3+}SiO_{12}$) (Fig. 6).

The analysis by μ-Raman also identified K-feldspars ($KAlSi_3O_8$) in the glaze-ceramic interface, which correspond to the acicular crystals observed in Fig. 4*b*. The strong band at 511 cm^{-1} and the weak band at 282 cm^{-1} characterise the spectrum of the K-feldspar (Fig. 6*d*), and the broad and weaker bands at 455 cm^{-1} and 472 cm^{-1} suggest the presence of either orthoclase or sanidine, or even an intermediate phase

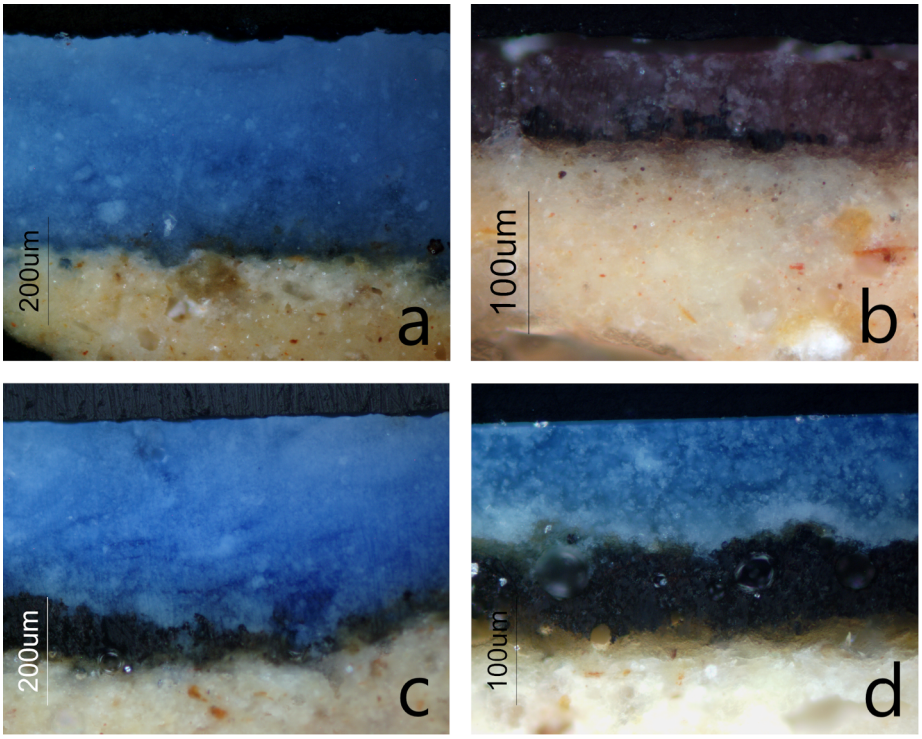

Fig. 3. Cross-section images obtained by OM, showing the coloured glaze and the glaze-ceramic body interface from samples: **(a)** MCV 2–1 T (blue); **(b)** MCV 1-1R (brown); **(c)** SCV 34Ei4068 (blue); **(d)** IVDJ-S 4134 (blue).

between these structural types of potassium feldspars (Freeman et al., 2008). K-feldspars (mostly sanidine) crystals have been previously identified in Islamic and Hispano-Moresque lead-glazed ceramics as the result of the reaction between lead-rich glazes and potassium-rich ceramic bodies at high temperatures (800–1000 °C) (Coentro et al., 2018; Molera et al., 1993; Pradell et al., 2010). The euhedral morphology indicates that these crystals are formed during the melting of the glaze. Their growth is also promoted by a slow cooling process (Molera et al., 1993).

The tin-rich inclusions observed by SEM in the glaze were confirmed to be cassiterite (SnO_2) by their strong Raman band at 633 cm^{-1} (Fig. 6*e*).

3.4. μ-PIXE analysis

The chemical composition of the glazes obtained by μ-PIXE is presented in Table 3. Silica (SiO_2) and lead oxide (PbO) are the major components of the white glaze, with contents of 36–46 wt% for SiO_2 and of 35–46 wt% for PbO. Sample MCV 3-1R is an exception with 54 wt% SiO_2 and 27 wt% PbO.

The third major component is tin oxide (SnO_2). The SnO_2 content of the white glaze is a distinctive factor among the three groups of samples, where the lowest values were identified for MCV tiles (3.7–4.5 wt % SnO_2), followed by SCV (6.4–7.8 wt% SnO_2) and IVDJ-S (7.8 – 8.6 wt % SnO_2).

Fig. 7 illustrates the positive correlation observed between SnO_2 and Na_2O for SCV and IVDJ-S groups, as well as a negative correlation between SnO_2 and PbO. MCV group, however, exhibits a small positive correlation between SnO_2 and K_2O. Furthermore, and apart from the MCV lower SnO_2 contents, K_2O is also a distinguishing factor between the IVDJ-S + SCV and MCV groups, with higher contents for the latter. This is observed both in white and in blue-coloured glazes.

The analysis of blue-decorated glazes by μ-PIXE identified cobalt in every sample (Table 3). A positive correlation is visible between Fe and Co, as well as between Ni and Co in most samples (Fig. 8). IVDJ-S samples contain higher Ni contents than the others. Copper was also identified in approximately half of the analysed glazes, without a specific connection to any of the studied groups.

Manganese was identified in samples MCV 1-1R and MCV 8-1G as responsible for the brown colour.

4. Discussion

4.1. Glaze composition

The analysis of the glaze compositions by μ-PIXE identified SnO_2 contents within expected values for Hispano-Moresque tin-glazed ceramics (Coentro et al., 2014, 2017; Molera et al, 1997, Molera et al., 2001; Pérez-Arantegui et al., 2005, 2009a; Polvorinos del Rio and Castaing, 2010). The white glaze in these underglaze-decorated tiles shows a similar composition to the one used for the other typologies in the same collections (Coentro et al., 2014, 2017). Also in accordance with these results, the homogeneity of the tin glazes follows the Islamic and Hispano-Moresque technology in what concerns the use of frits (Allan, 1973; Molera et al., 2009), although the larger size of cassiterite crystals observed in IVDJ-S and SCV groups suggest a lower degree of grinding than the one observed for MCV glazes.

The positive correlation between sodium and tin oxides, as well as a negative correlation between lead and tin oxides visible in Fig. 7 for SCV and IVDJ-S samples, suggest that – in these two sets – tin was added to the glaze recipe together with a sodium-rich flux, but not with lead, contrarily to what is mentioned in the Persian treatise from 1301 by Abu l'Qasim (Allan, 1973) or in the Italian treatise on majolica by Cipriano Piccolpasso (*ca.* 1557) (Piccolpasso, 1980). They are, however, in accordance with the results obtained by Molera et al. (2009) from the analysis of frits found in archaeological context in a medieval kiln in Paterna.

The difference in potassium contents has been previously identified in a study comparing Sevillian and Valencian lustre-decorated ceramics (Polvorinos del Rio and Castaing, 2010). The higher potassium content in MCV glazes is likely a consequence of several factors, such as its higher content in the sand used as a silica source for the glaze and the

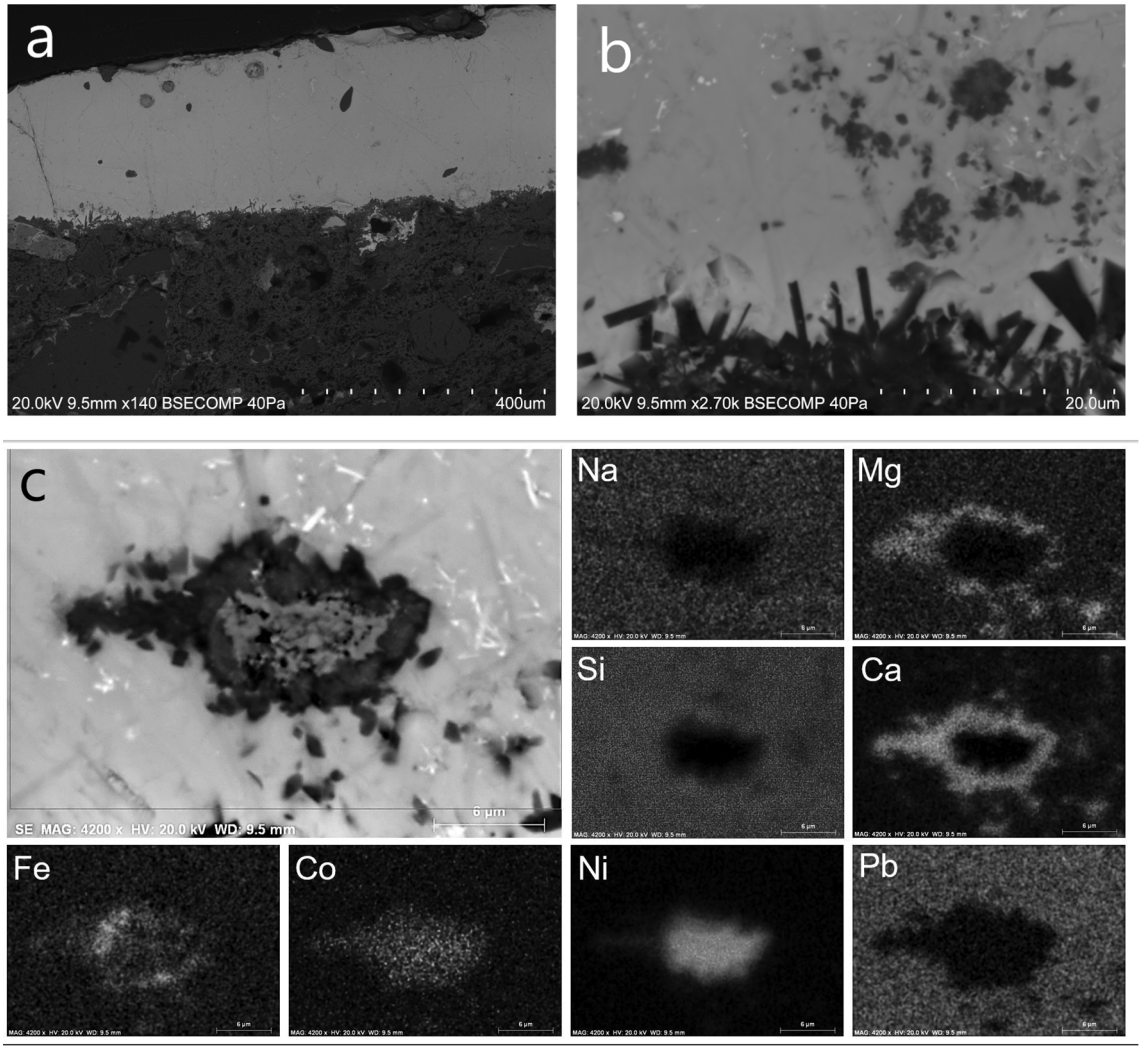

Fig. 4. (a) SEM-BSE cross-section image illustrating *Type 1* glaze morphology (MCV 4-2G), exhibiting a homogeneous glaze with few inclusions; **(b)** detail of the glaze-ceramic interface where Co-rich particles are observed above it; **(c)** detail of a cobalt pigment particle where different areas are observed, and its EDS elemental maps for Na, Mg, Si, Ca, Fe, Co, Ni, and Pb.

reaction with the also K-rich clay in the ceramic body, since the latter also presents higher potassium values in its composition (Coentro, 2017). On the other hand, potassium could be added as a flux obtained from ashes of forest plants or wine lees (Piccolpasso, 1980; Tite et al., 2006), but the source is difficult to determine in a glaze due to the influence of the ceramic body in its final composition.

4.2. Cobalt blue pigment

The Fe-Co-Ni-Cu association identified in approximately half of the blue samples fits within the expected chemical composition in Hispano-Moresque ceramics dated until the beginning of the 16th century. Adding to Hispano-Moresque cuerda-seca and arista blue glazes (Coentro et al., 2014, 2017; Fares et al., 2012), the association between copper and cobalt has been identified in coeval blue-decorated ceramics from Teruel and Manises-Paterna (Pérez-Arantegui et al., 2009b; Resano et al., 2005; Roldán et al, 2006), in Renaissance Della Robbia glazes dated prior to *ca.* 1520 (Zucchiatti et al., 2006) and in an Islamic 17th century tile panel in Northern India (Gill and Rehren, 2011).

This period is also associated with the "absence" of arsenic in the pigment composition, or, in other words, with arsenic contents in trace amounts, only detected by highly sensitive analytical techniques. This explains why "needle-like" As-rich structures mentioned in the literature for other Co-blue glazes (Guilherme et al., 2014; Zucchiatti et al., 2006) were not observed in these tiles, nor was As detected by µ-PIXE analysis.

The morphology of the pigment particles, with their Fe-Co-Ni-rich nuclei, is similar to other previously identified in a coeval arista tile (Coentro et al., 2018), as is the outer layer rich in Si, Ca, Mg and Na illustrated in Fig. 3*c*. Another parallel morphology was found in Chinese ceramics (Jiang et al., 2018), where the cobalt pigment was identified "encapsulated" within anorthite clusters. Several hypotheses may explain the presence of Si, Ca, Mg and Na surrounding the blue pigment particles: it could be a result from the reaction between the pigment and the ceramic body of the tiles; or the cobalt pigment already had these elements in its composition if it was prepared and exported as zaffre, which was obtained by roasting the cobalt ore with sand (Mimoso, 2015); or, finally, it could result from an intentional mixture of the pigment with clay, which has been reported for Chinese ceramics as a technique for preventing the blue colour from spreading (Jiang et al., 2018). On the other hand, the previously mentioned arista tile does not have underglaze decoration and its blue glaze is homogeneously coloured with a cerulean blue shade. Considering the similarity between its pigment particles and the ones observed in this study, it seems more likely that the cobalt pigment was already mixed with sand or clay prior to its use on the tile (either to paint directly on it or to mix with a glaze frit).

The two types of glazes identified in this study suggest two different ways of applying the cobalt pigment under tin-opacified glazes. While

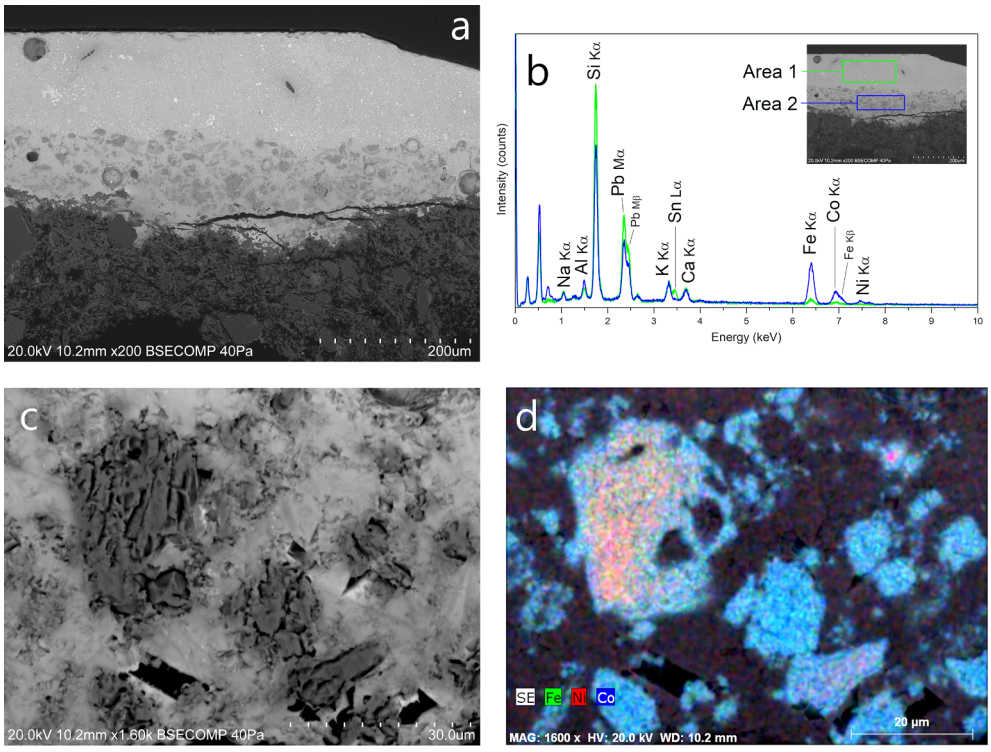

Fig. 5. (a) SEM-BSE cross-section image illustrating *Type 2* glaze morphology (SCV 49-15F4338), where an intermediate layer corresponding to the Co-blue pigment stands out between the ceramic body and the upper tin-opacified glaze; **(b)** EDS analysis of the two different layers observed in (a); **(c)** detail of cobalt pigment particles from the lower layer in (a); **(d)** EDS map of the particles observed in (c).

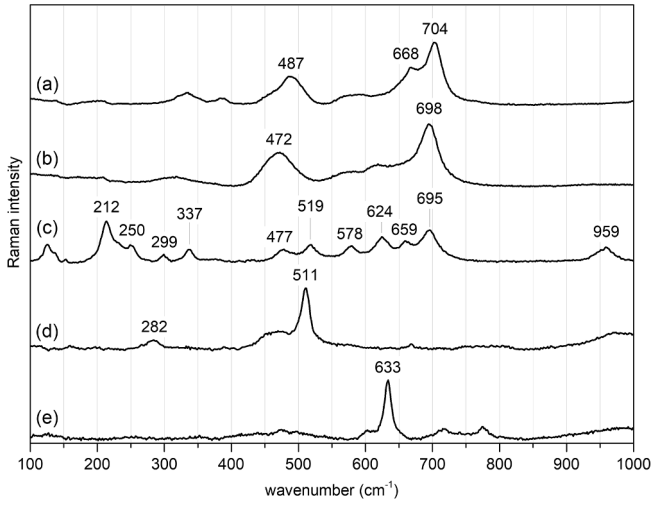

Fig. 6. µ-Raman spectra of the compounds identified in the glazes: **(a)** Ni-Co ferrite (487 and 704 cm^{-1}) and magnetite (668 cm^{-1}) (MCV 2-1T); **(b)** Ni ferrite ($NiFe_2O_4$) (SCV 34Ei4068); **(c)** braunite and hausmannite, the latter represented by the band at 659 cm^{-1} (MCV 1-1R); **(d)** potassium feldspar ($KAlSi_3O_8$) (MCV 2-1T); **(e)** cassiterite (SnO_2) (SCV 34Ei4068).

there is archaeological evidence of the application of the cobalt blue pigment on raw ceramic bodies in Valencia, the decoration process of Sevillian underglaze-decorated ceramics is still unknown. From the results obtained in this study, it is not clear if the Sevillian-attributed samples were decorated prior to biscuit-firing. Also, further experiments (namely reproductions and their respective analysis) will be necessary to understand why such a thick pigment layer was used in these tiles, especially considering the high cost of cobalt at the time.

4.3. Manganese brown

Manganese was identified in the form of braunite in samples MCV 1-1R and MCV 8-1G in association with the brown colour. This result is consistent with other tin-opacified manganese brown-decorated ceramics from the Iberian Peninsula from the 11th century onwards (Coentro et al., 2012, 2018; Coutinho et al., 2016; Molera et al., 2013; Pradell et al., 2010).

Braunite may result from the reaction between a manganese oxide used as a pigment – such as pyrolusite (MnO_2) or hausmannite ($Mn^{2+}Mn_2^{3+}O_4$) – and the glaze matrix above 1000 °C (Molera et al, 2013). The manganese ore could also have been calcined with clay or sand prior to its application on the tile, in which case braunite was already formed before the final firing and should not be used as a temperature marker. However, the SEM images obtained in this study reveal homogeneous pigment particles without any visible layers such as the ones present in the cobalt blue pigment.

5. Conclusion

In this study, two types of tin-opacified underglaze decoration were identified, allowing the distinction between Valencian and Sevillian tiles: *Type 1* is observed for flat Valencian tiles and characterised by small Co– or Mn-rich particles (< 15 µm) scarcely distributed near the glaze-ceramic interface; *Type 2* was identified in *arista* and "low-*arista*" Sevillian (or Sevillian-attributed) tiles and is characterised by two distinct layers, where the lower one is composed of many inclusions related to the Co pigment, and the upper layer is more homogeneous and similar to the MCV glazes with its well-distributed tin oxide agglomerates.

Further differences were identified in the chemical composition of the tin-glaze: *Type 1* glazes exhibit lower SnO_2 and higher K_2O contents than *Type 2* glazes, suggesting that different glaze recipes were used in the two production centres.

The chemical composition of the cobalt blue pigment fits within the expected Fe-Co-Ni-Cu association, without As, identified in Hispano-Moresque ceramics until the beginning of the 16th century. The morphology of the pigment particles exhibits a Fe-Co-Ni-rich nucleus with an outer layer rich in Si, Ca, Mg and Na, which may result from a prior mixture of the blue pigment with sand (as *zaffre*) or with clay.

According to the cited literature, blue-and-white underglaze-

Table 3
Chemical composition of the glazes obtained by μ-PIXE.

	NaO	MgO	Al_2O_3	SiO_2	Cl	K_2O	CaO	TiO_2	MnO	Fe_2O_3	CoO	NiO	CuO	SnO_2	PbO
White															
MCV 2-1T	1.17	0.35	1.39	42.1	0.82	4.54	1.67			0.26				4.50	43.2
MCV 3-1R	1.58	0.66	2.32	54.2	0.33	6.37	2.83	0.08		0.52				4.10	27.0
MCV 4-1G	1.83	0.36	2.07	46.4	0.52	3.42	2.15	0.06		0.35				3.97	38.9
MCV 4-2G	1.87	0.28	2.25	43.5	0.98	3.69	1.85			0.46				3.71	41.4
MCV 8-1G	2.34	0.42	1.51	45.0	0.87	4.60	1.76			0.17				4.07	39.2
SCV 51-1M4467	2.38	0.58	2.21	42.3	0.34	2.64	2.62	0.14		0.73				7.67	38.4
SCV 34Ei4068	1.85	0.35	1.57	41.0	0.66	3.15	2.13	0.13		0.95			0.12	6.65	41.4
SCV 494i4327	2.25	0.53	1.69	43.9	0.51	3.11	2.72	0.13		0.51				7.75	36.9
SCV 49-15F4338	1.66	0.35	1.68	35.9	0.42	2.82	2.98	0.18		2.12				6.35	45.5
IVDJ-S 4134	2.43	0.51	2.51	42.7	0.30	3.53	2.65	0.14	0.02	0.53			0.04	7.84	36.8
IVDJ-S 4185	2.82	0.88	2.46	43.0	0.45	2.71	3.43	0.14		0.71			0.06	8.58	34.7
Blue															
MCV 2-1T	1.41	0.33	1.52	42.6	1.14	4.58	1.46			0.46	0.16			4.10	42.2
MCV 3-1R	1.72	1.05	2.10	50.4	0.30	6.27	3.02	0.08	0.34	0.88	0.39	0.18		4.71	28.6
MCV 8-1G	3.45	0.39	1.62	45.6	1.00	4.40	1.85	0.06		0.63	0.16	0.12		4.16	36.6
MCV 8-2C	1.63	0.68	2.73	52.5	0.17	5.64	3.75	0.39	0.18	3.52	1.20	0.32	0.08	4.38	22.9
MCV 8-3G	1.22	0.37	2.03	45.7	0.47	5.76	2.21		0.09	3.68	1.00	0.31	0.28	4.66	32.2
SCV 51-1M4467	2.33	0.49	1.84	40.7	0.78	2.07	2.81	0.17		1.64	0.34			6.95	39.9
SCV 34Ei4068	2.27	0.39	1.67	41.9	0.58	3.19	2.04	0.16		2.57	0.98	0.22	0.32	7.55	36.2
SCV 494i4327	1.73	0.47	1.78	40.1	0.50	3.35	2.45	0.11	0.04	4.51	1.47	0.36	0.13	8.31	34.7
SCV 49-15F4338	1.97	0.37	2.01	39.3	0.42	3.55	2.90	0.14		3.02	1.05			6.93	38.3
IVDJ-S 4134	2.24	0.51	3.14	40.6	0.19	3.59	2.68	0.16	0.06	3.58	1.22	0.48	0.94	9.69	31.0
IVDJ-S 4185	3.60	1.52	4.72	45.9	0.10	2.81	6.52	0.22	0.05	4.06	1.27	0.58		5.48	23.2
Brown															
MCV 1-1R	1.47	0.36	2.37	40.5	0.75	4.39	2.05	0.13	3.74	0.68				4.73	38.8
MCV 8-1G	2.42	0.43	1.57	42.1	0.88	4.43	1.99	0.06	2.73	0.51				4.58	38.3

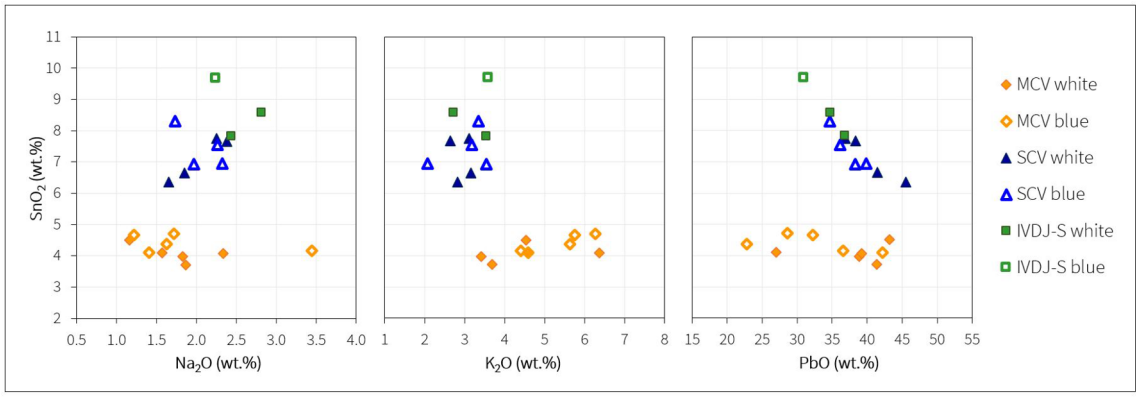

Fig. 7. Scatter plots of SnO_2 vs. Na_2O, K_2O and PbO, obtained by μ-PIXE.

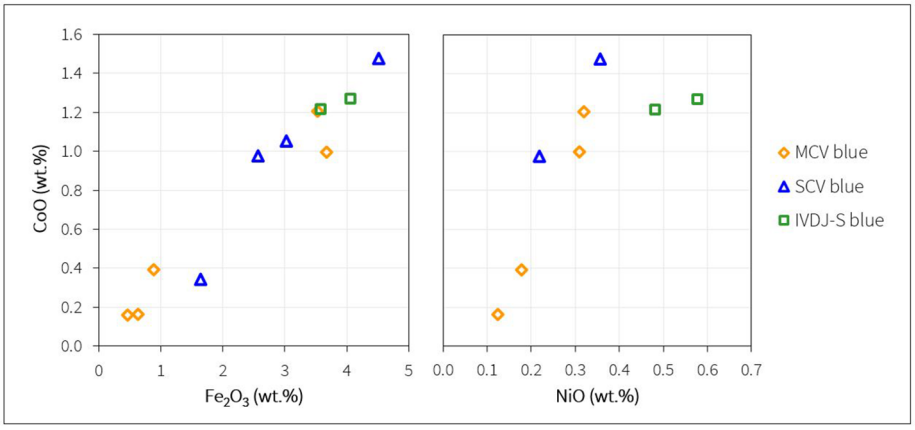

Fig. 8. Scatter plots of CoO vs. Fe_2O_3 and NiO, obtained by μ-PIXE.

decorated tin-opacified ceramics have been identified in Hispano-Moresque production centres in the Valencian region, in Seville, and in an Islamic production from Granada. Although it is likely that this technology has an Islamic origin, it has not been – at the time of this publication – documented outside the Iberian Peninsula. The closest technological parallels would be the Islamic 9th-10th-century underglaze-decorated wares from Sicily (Testolini 2018), although these were not tin-opacified, or Iznik ceramics, where a lead-alkali glaze with a considerable amount of tin oxide (*ca.* 3–8.5 wt%) was used over the coloured decorations. However, most of the tin oxide in Iznik ware is in solution in the glaze, making it basically transparent (Paynter et al., 2004). Although this transparency was important to reveal the underglaze decoration in Iznik ceramics, the same does not apply when only cobalt and manganese pigments are used, as the Valencian and Sevillian underglaze-decorated tin-opacified ceramics attest.

CRediT authorship contribution statement

S. Coentro: Conceptualization, Investigation, Writing - original draft, Writing - review & editing, Visualization. **L.C. Alves:** Investigation, Writing - review & editing. **J. Coll Conesa:** Resources, Writing - review & editing. **T. Ferreira:** Investigation, Writing - review & editing. **J. Mirão:** Investigation, Writing - review & editing. **R.C. da Silva:** Supervision, Writing - review & editing. **R. Trindade:** Supervision, Writing - review & editing. **V.S.F. Muralha:** Supervision, Conceptualization, Methodology.

Acknowledgements

The authors would like to thank Dr Manuela Fonseca, Dr Artur Côrte-Real and Dr Catarina Leal from Monastery of Santa Clara-a-Velha (Coimbra, Portugal), and Dr Elisa Ramiro and Dr Cristina Partearroyo from the Instituto Valencia de Don Juan (Madrid, Spain), for allowing and encouraging the study of their collections.

A special acknowledgement to Dr João Manuel Mimoso, to Prof. Hans van Lemmen, and to Dr Trinitat Pradell, for providing information and very interesting discussions regarding the cobalt blue pigment and its application. Also, to Dr Oliver Watson and Dr Véronique François, whose clarifications helped our *state-of-the-art* revision.

To our anonymous Reviewers, we thank you for your comments and suggestions, which contributed to an improved final version of this paper.

Funding

Fundação para a Ciência e Tecnologia (Portugal): CEECIND/00882/2017 (S. Coentro); UIDB/00729/2020 (VICARTE); UID/Multi/04449/2013 (CT2N-IST-UL). INALENTEJO/QREN/FEDER (Portugal): LARES (ALENT-07-0224-FEDER-001761) and MICRA.Lab (ALENT-07-0262-FEDER-001868) projects.

References

Allan, J.W., 1973. Abu'l-Qasim's treatise on ceramics. Iran 11, 111–120.

Arcifa, L., Bagnera, A. (2018). Palermo in the Ninth and Early Tenth Century: Ceramics as Archaeological Markers of Cultural Dynamics. In: Anderson, G.D., Fenwick, C., & Rosser-Owen, M. (Eds), The Aghlabids and their Neighbors: Art and Material Culture in Ninth-Century North Africa. Series: Handbook of Oriental Studies. Section 1 The Near and Middle East, Vol. 122, p. 382–404.

Ben Amara, A., Schvoerer, M., Daoulatli, A., Rammah, M., 2011. "Jaune de Raqqada" et autres couleurs de céramiques glaçurées aghlabides de Tunisie (IX^{e}-X^{e} siècles). Revue d'Archéometrie 25, 179–186.

Brill, R.H., 1999. Chemical Analysis of Early Glasses. The Corning Museum of Glass, Corning, New York.

Campbell, J.L., Boyd, N.I., Grassi, N., Bonnick, P., Maxwell, J.A., 2010. The Guelph PIXE Software Package IV. Nucl. Instrum. Methods B 268, 3356–3363.

Chandramohan, P., Srinivasan, M.P., Velmurugan, S., Narasimhan, S.V., 2011. Cation distribution and particle size effect on Raman spectrum of $CoFe_2O_4$. J. Solid State Chem. 184, 89–96.

Coentro, S., Lima, A.M., Silva, A.S., Pais, A.N., Mimoso, J.M., Muralha, V.S.F., 2012. Pigments and pigment mixtures in Portuguese 17th century Azulejos. J. Eur. Ceram. Soc. 32 (1), 37–48.

Coentro, S., Trindade, R.A.A., Mirão, J., Candeias, A., Alves, L.C., da Silva, R.C., Muralha, V.S.F., 2014. Hispano-Moresque ceramic tiles from the Monastery of Santa Clara-a-Velha (Coimbra, Portugal). J. Archaeol. Sci. 41, 21–28.

Coentro, S., Alves, L.C., Relvas, C., Ferreira, T., Mirão, J., Molera, J., Pradell, T., Trindade, R.A.A., da Silva, R.C., Muralha, V.S.F., 2017. Glaze technology of hispano-moresque ceramic tiles: a comparison between Portuguese and Spanish collections. Archaeometry 59 (4), 667–684.

Coentro, S., 2017. An Iberian Heritage: Hispano-Moresque Architectural Tiles in Portuguese and Spanish Collections. PhD Thesis. Universidade Nova de Lisboa.

Coentro, S., Relvas, C., Ferreira, T., Mirão, J., Trindade, R.A.A., Pleguezuelo, A., da Silva, R.C., Muralha, V.S.F., 2018. Mineralogical characterization of hispano-moresque glazes: a μ-Raman and scanning electron microscopy with X-ray energy dispersive spectrometry (SEM-EDS) study. Microsc. Microanal. 24 (3), 300–309.

Coll Conesa, J., 2009a. Cobalt blue in medieval ceramic production in the Valencian workshops. Manises, Paterna and Valencia, Spain. Medieval Ceram. 31, 11–24.

Coll Conesa, J., 2009b. *La Cerámica Valenciana: Apuntes para una síntesis.* Asociacion Valenciana de Cerámica. Avec-Gremio/RM Ediciones, Valencia.

Coutinho, M.L., Veiga, J.P., Alves, L.C., Mirão, J., Dias, L., Lima, A.M., Muralha, V.S., Macedo, M.F., 2016. Characterization of the glaze and in-glaze pigments of the nineteenth-century relief tiles from the Pena National Palace, Sintra, Portugal. Appl. Phys. A 122, 696.

Fares, M., Pais, A.N., Martins, I.M., Coentro, S., Pereira, S., Muralha, V., Mimoso, J.M., 2012. *Azulejo blues – an analytic study of the blue shades in Portuguese azulejos*, Proceedings of the International Congress AZULEJAR, 10–12th October 2012. Aveiro, Portugal.

Freeman, J.J., Wang, A., Kuebler, K.E., Jolliff, B.L., Haskin, L.A., 2008. Characterization of natural feldspars by Raman spectroscopy for future planetary exploration. Can. Mineral. 46 (6), 1477–1500.

García-Porras, A. (2012), El azul en la producción cerámica bajomedieval de las áreas islámica y cristiana de la Península Ibérica, IX Congreso Internacional de Cerámica Medieval en el Mediterráneo, Florencia, 2012.

Gill, M.S., Rehren, T., 2011. Material characterization of ceramic tile mosaics from two 17th century Islamic monuments in northern India. Archaeometry 53, 22–36.

Grime, G.W., Dawson, M., 1995. Recent developments in data acquisition and processing on the oxford scanning proton microprobe. Nucl. Instrum. Methods B 104, 107–113.

Guilherme, A., Hodoroaba, V.D., Benemann, S., Coroado, J., Carvalho, M.L., 2014. Morphological and compositional features of blue and yellow pigments used in Portuguese glazed ceramics by SEM/EDX – unravelling manufacturing differences. J. Anal. At. Spectrom. 29, 51–57.

Jiang, X., Ma, Y., Chen, Y., Li, Y., Ma, Q., Zhang, Z., Wang, C., Yang, Y., 2018. Raman analysis of cobalt blue pigment in blue and white porcelain: a reassessment. Spectrochim. Acta Part A Mol. Biomol. Spectrosc. 190, 61–67.

Kamble, R.B., Varade, V., Ramesh, K.P., Prasad, V., 2015. Domain size correlated magnetic properties and electrical impedance of size dependent nickel ferrite nanoparticles. AIP Adv. 5 (1), 17119.

Kim, J., Choi, K.J., Bahn, C.B., Kim, J.H., 2014. In situ Raman spectroscopic analysis of surface oxide films on Ni-base alloy/low alloy steel dissimilar metal weld interfaces in high-temperature water. J. Nucl. Mater. 449, 181–187.

Majumdar, M.G., 2012. Analysis of stress-coupled magneto-electric effect in $BaTiO_3$-$CoFe_2O_4$ composites using Raman Spectroscopy. Int. J. Sci. Eng. Res. 3 (11).

Martínez Caviró, B., 1991. Cerámica Hispanomusulmana andalusí y mudéjar. Ediciones El Viso, Madrid.

Matin, M., Tite, M., Watson, O., 2018. On the origins of tin-opacified ceramic glazes: New evidence from early Islamic Egypt, the Levant, Mesopotamia, Iran, and Central Asia. J. Archaeol. Sci. 97, 42–66.

J.M. Mimoso Origin, early history and technology of the blue pigment in azulejos 2015 Lisbon, Portugal.

Molera, J., Pradell, T., Martinez-Manent, S., Vendrell-Saz, M., 1993. The growth of sanidine crystals in the lead of glazes of Hispano-Moresque pottery. Appl. Clay Sci. 7 (6), 483–491.

Molera, J., Pradell, T., Merino, L., García-Vallés, M., García-Orellana, J., Salvadó, N., Vendrell-Saz, M., 1997. La tecnología de la cerámica Islámica y Mudéjar. Caesaraugusta 73, 15–41.

Molera, J., Vendrell-Saz, M., Pérez-Arantegui, J., 2001. Chemical and textural characterization of tin glazes in Islamic ceramics from Eastern Spain. J. Archaeol. Sci. 28, 331–340.

Molera, J., Pradell, T., Salvadó, N., Vendrell-Saz, M., 2009. Lead Frits in Islamic and Hispano-Moresque glazed productions. In: Shortland, A.J., Freestone, I., Rehren, T. (Eds.), From Mine to Microscope: Advances in the study of Ancient Technology. Oxbow Books, Oxford, pp. 1–10.

Molera, J., Coll, J., Labrador, A., Pradell, T., 2013. Manganese brown decorations in 10th to 18th-century Spanish tin glazed ceramics. Appl. Clay Sci. 82, 86–90.

Paynter, S., Okyar, F., Wolf, S., Tite, M.S., 2004. The production technology of Iznik pottery – a reassessment. Archaeometry 46, 421–437.

Pérez-Arantegui, J., Ortega, J.M., & Escriche, C. (2005). La tecnología de la cerámica Mudéjar entre los siglos XIV y XVI: las producciones esmaltadas de las zonas de Teruel y Zaragoza, VI Congreso Ibérico de Arqueometría: Avances en Arqueometría, 89–96.

Pérez-Arantegui, J., Ortega, J., Escriche, C., 2009a. The Hispano-Moresque tin glazed ceramics produced in Teruel, Spain: a technology between two historical periods, 13th to 16th c. AD. In: Shortland, A.J., Freestone, I., Rehren, T. (Eds.), From Mine to Microscope: Advances in the study of Ancient Technology. Oxbow Books, Oxford, pp. 61–67.

Pérez-Arantegui, J., Montull, B., Resano, M., Ortega, J.M., 2009b. Materials and technological evolution of ancient cobalt-blue-decorated ceramics: Pigments and work patterns in tin-glazed objects from Aragon (Spain) from the 15th to the 18th century AD. J. Eur. Ceram. Soc. 29 (12), 2499–2509.

Piccolpasso, C., 1980. *The Tree Books of Potter's Art (Il Tre Libri Dell'Arte Del Vasaio)* – A Facsimile of the Manuscript in the Victoria and Albert Museum [*Translated by Alan Caiger-Smith*]. Scholar Press, London.

Pleguezuelo, A., 2011. Lozas y azulejos de Triana – Coleccion Carranza. Ayto, Sevilla.

Polvorinos del Rio, A., Castaing, J., 2010. Lustre-Decorated Ceramics from a 15th to 16th Century Production in Seville. Archaeometry 52 (1), 83–98.

Pradell, T., Molera, J., Salvadó, N., Labrador, A., 2010. Synchrotron radiation micro-XRD in the study of glaze technology. Appl. Phys. A 99, 407–417.

Resano, M., Pérez-Arantegui, J., García-Ruiz, E., Vanhaecke, F., 2005. Laser ablation-inductively coupled plasma mass spectrometry for the fast and direct characterization of antique glazed ceramics. J. Anal. At. Spectrom. 20, 508–514.

Roldán, C., Coll, J., Ferrero, J., 2006. EDXRF analysis of blue pigments used in Valencian ceramics from the 14th century to modern times. J. Cult. Heritage 7, 134–138.

RRUFF Project Database. [http://rruff.info/] (last accessed 02-03-2018).

Salinas, E., Molera, J., and Pradell, T. (2017). Evolución de la cerámica "verde y manganeso" en la península Ibérica desde las primeras producciones islâmicas (finales del siglo IX-principios del siglo X) hasta las producciones bajomedievales cristianas (siglos XIII-XIV). In: Actas del XII Congreso Ibérico de Arqueometria, Burgos, España, p. 66.

Salinas, E., Pradell, T., 2018. The transition from lead transparent to tin-opacified glaze productions in the western Islamic lands: al-Andalus, c. 875–929 CE. J. Archaeol. Sci. 94, 1–11.

Testolini, V. (2018). Ceramic Technology and Cultural Change in Sicily from the 6th to the 11th centuries AD). PhD Thesis. University of Sheffield, UK.

Tite, M.S., Shortland, A., Maniatis, Y., Kavoussanaki, D., Harris, S.A., 2006. The composition of the soda-rich and mixed alkali plant ashes used in the production of glass. J. Archaeol. Sci. 33, 1284–1292.

Tite, M.S., Wolf, S., and Mason, R.B. (2011). The technological development of stonepaste ceramics from the Islamic East, J. Archaeol. Sci. 38: 570–580.

Watson, O., 2004. Ceramics from Islamic Lands. Thames & Hudson, London.

Zucchiatti, A., Bouquillon, A., Katona, I., & D'Alessandro, A. (2006). The 'Della Robbia blue': a case study for the use of cobalt pigments in ceramics during the Italian Renaissance, Archaeometry, 48 (1), 131–152.